Journal of Catalysis 268 (2009) 9–17

Contents lists available at ScienceDirect

Journal of Catalysis

journal homepage: www.elsevier.com/locate/jcat

The benefit of multipore zeolites: Catalytic behaviour of zeolites with intersecting channels of different sizes for alkylation reactions

Avelino Corma [a,*], Francisco J. Llopis [b], Cristina Martínez [a], Germán Sastre [a], Susana Valencia [a]

[a] Instituto de Tecnología Química U.P.V.-C.S.I.C., Universidad Politécnica de Valencia, Avenida Los Naranjos s/n, 46022 Valencia, Spain
[b] Departamento Ingeniería Química, U.V.E.G., Universidad de Valencia, Burjassot, Valencia, Spain

ARTICLE INFO

Article history:
Received 5 May 2009
Revised 13 July 2009
Accepted 27 August 2009
Available online 8 October 2009

Keywords:
Multipore zeolites
Benzene alkylation with alcohols
Al distribution and proton location in zeolites
Selectivity with multipore zeolites
Ethylbenzene
Cumene

ABSTRACT

The catalytic behaviour of two multipore zeolites containing channels of different sizes, SSZ-33 (10 windows × 12 MR) and ITQ-22 (8 × 10 × 12 MR pores), for alkylation of benzene with ethanol and benzene with isopropanol or propylene, has been studied and compared to that of zeolites with intersecting channels of the same size, ZSM-5 (10 × 10 MR channels) and Beta (12 × 12 MR channels), which are industrially used for the above-mentioned process.

For the alkylation of benzene with ethanol in gas phase, ITQ-22 behaves like the 10 MR ZSM-5 with respect to ethylbenzene selectivity, while the behaviour of SSZ-33 is close to that of a 12 MR zeolite such as Beta. For the alkylation of benzene with isopropanol or propylene in gas and liquid phase, Beta and ITQ-22 give similar selectivity values, which are much better than those obtained with ZSM-5. Meanwhile, SSZ-33 gives intermediate selectivity between that of the 10 MR ZSM-5 and the 12 MR Beta zeolite.

ITQ-22, therefore, shows a unique behaviour as a multipurpose alkylation catalyst, with characteristics different from those of previously studied zeolites. The catalytic behaviour of ITQ-22 has been rationalized not only in terms of the topology of the channels but also taking into account the location of the protons. A computational study shows preferential Al location at the 10 MR, near the intersection with the 12 MR channels, and at the intersections between 10 and 12 MR channels.

1. Introduction

Zeolites were first introduced as acid catalysts for oil refining in the late 60s, improving the catalytic behaviour of the previous amorphous silica–alumina [1–4]. Zeolites, by having a defined micropore structure, were not only able to select the reactants that could enter the micropore, but also allowed the control of the acidic properties in terms of number, strength and location of the acid sites [5–7]. Micropore channels have unique features that can be classified by descriptors defined by the IZA (International Zeolite Association) [8]. Those descriptors are (i) size, in terms of number of tetrahedral atoms forming the rings controlling diffusion through the channels, (ii) size, in terms of channel dimensions or free diameter, and (iii) channel crystallographic directions. Intersections between channels, which may or may not form cavities, are also of great importance. All these factors, taken together, help to explain the results of catalytic activity as a function of micropore topology.

Multiple channel dimensionality (channels interconnected in 2-D or 3-D systems) is an important requirement for many reactions that find a benefit from the larger diffusivity that is allowed when channels intersect each other. In fact, most of the early commercial applications of zeolites employed zeolites containing 3-D micropores such as FAU, MFI and BEA. The channels in these three structures are formed by 12-membered rings (MR) for FAU and BEA, and by 10 MR for MFI. A different class of multipore zeolites appears when channels are of different sizes, and in this case a new concept called 'molecular traffic' [9] refers to the selectivity of different molecules to diffuse through different channels.

Examples of zeolites (with their corresponding topology indicated by the three-letter IZA code [8]) containing connected pores with different dimensions include: Ferrierite (FER, 8 × 10 MR) [10], ITQ-13 (ITH, 9 × 10 MR) [11], Mordenite (MOR, 8 × 12 MR) [12], Nu-87 (NES, 10 × 12 MR) [13], SSZ-33 (CON, 10 × 12 MR) [14], ITQ-22 (IWW, 8 × 10 × 12 MR) [15], IM-12/ITQ-15 (UTL, 12 × 14 MR) [16] and ITQ-33 (10 × 18 MR) [17]. The catalytic benefit of zeolites containing more than one type of pores within the same structure has been shown for reactions such as the isomerization of 1-butene into isobutene in ferrierite [18,19], where the preferential location of acid sites was crucial, the dealkylation–transalkylation of heavy naphtha in Nu-87, SSZ-33 and ITQ-23 [20–22], the carbonylation of dimethyl-ether and methanol with CO in Mordenite [23–25], and the catalytic cracking of a VGO on ITQ-33-based catalysts, with the resulting maximization of diesel and propylene yields [17,26].

* Corresponding author. Fax: +34 96 387 7809.
E-mail address: acorma@itq.upv.es (A. Corma).

0021-9517/$ - see front matter © 2009 Elsevier Inc. All rights reserved.
doi:10.1016/j.jcat.2009.08.012

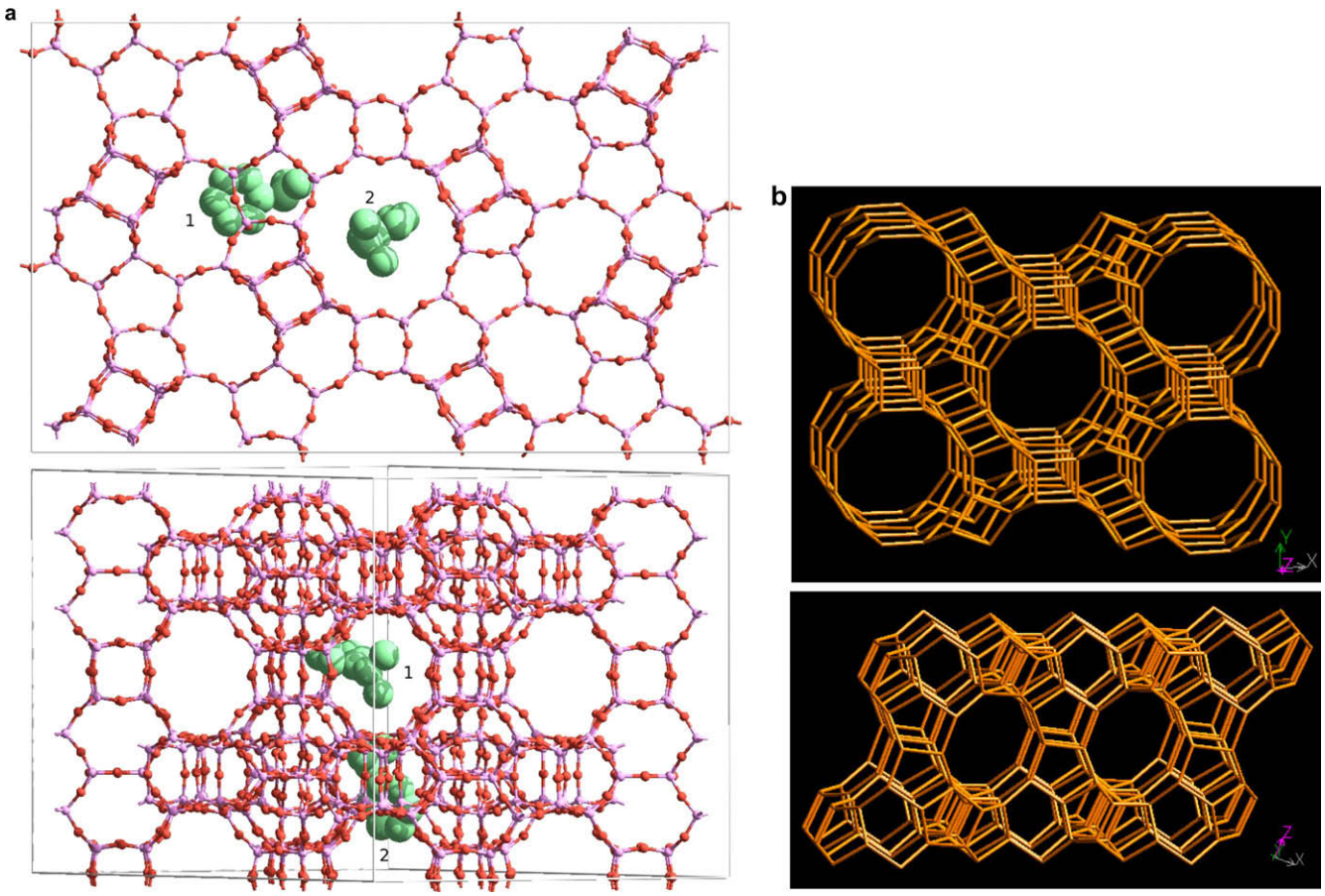

Fig. 1. (a) ITQ-22 with 2 cumene molecules (hydrogens not shown for clarity) in relative minimum energy locations. Cumene '1' is in the 10 MR system and cumene '2' is in the 12 MR channel. Both locations are energetically favourable. Top: view across [0 0 1]. Bottom: view across [1 1 0]. (b) Structure of SSZ-33 zeolite (CON) taken from http://www.iza-structure.org/. Top: framework viewed along [0 0 1]. Bottom: framework along [0 1 0].

When discussing on multipore zeolites, we have found it useful to differentiate the structures with defined pores from the structures in which one of the pores corresponds more to a window (or a short segment) than to a non-intersected channel. For example, the 2-D 10×10 channel system of NES generates cavities whose size is equivalent to 12 MR. In this sense, the channels of NES can be considered 10×12 MR instead of 10×10 MR, and the topology of this channel system is very different from that of a typical 10×10 channel system such as the MFI. Thus, in multipore zeolites, a careful inspection of the micropore topology is required in order to properly relate the catalytic results with the channel systems.

Along these lines, another example is SSZ-33 [14], which could be, in principle, considered as a zeolite with 10 and 12 MR pores, but would be better defined as a zeolite with 12 MR pores connected by 10 MR windows. Also, ITQ-27 [27] should be defined as formed by 12 MR channels connected by 14 MR windows.

We have investigated here the catalytic behaviour of two multipore zeolites, i.e., SSZ-33 (10 windows $\times$ 12 MR) and ITQ-22 ($8 \times 10 \times 12$ MR pores, see Fig. 1) with respect to two reactions, namely the alkylations of benzene with ethanol and of benzene with isopropanol and propylene, which not only are of industrial interest, but also are very useful as test reactions for studying zeolite topology [28,29]. When working in vapour phase conditions, the first reaction is better catalysed by 10 MR zeolites, while the second one requires the use of 12 MR zeolites. As a reference catalyst for these two reactions, we have used ZSM-5 (MFI topology) and Beta (BEA topology) zeolites, with 10×10 and 12×12 MR pores, respectively, which are of industrial relevance for those two alkylation reactions [30–34].

Our study arose from the following consideration: How would SSZ-33 and ITQ-22 behave from the selectivity point of view, as a 10 MR, as a 12 MR zeolite, or as something in between? Taking into account the respective pore topologies, our initial hypothesis was that SSZ-33 should behave more like a 12 MR zeolite since the 10 MR are windows rather than channels. However, in the case of ITQ-22, with discrete 10 and 12 MR pores, we could not guess whether the effect of any of the two pore systems would predominate, or it would behave as a 10 MR for ethylbenzene formation and as a 12 MR for cumene production. If the latter was true, ITQ-22 would show a unique behaviour as a multipurpose alkylation catalyst.

2. Experimental

2.1. Catalyst preparation

Highly crystalline ITQ-22 was obtained as described in previous work [15]. The organic structure directing (SDA) cation 1,5-bis-(methylpyrrolidinium)-pentane (MPP) was obtained by reacting an excess of *N*-methylpyrrolidine (97%, Aldrich) with 1,5-dibromopentane (97%, Aldrich) in acetone under reflux for 24 h. The resulting solid was separated by careful decantation, and it was then exhaustively washed with acetone until the unreacted amine was completely removed from the solid.

The solid was characterized as $MPPBr_2$ by elemental analysis (exp: 44.09 wt% C, 8.51 wt% H, 6.84 wt% N, 40.56 wt% Br; calc: 45.02 wt% C, 8.06 wt% H, 7.00 wt% N, and 39.92 wt% Br) and ^1H NMR. The product was dissolved in water and anion exchanged with DOWEX resin to yield a solution of the dihydroxide form of MPP cation, which was used as the organic structure directing agent in the synthesis gel.

Al-containing ITQ-22 was synthesized from a starting mixture of composition:

0.66 SiO_2:0.33 GeO_2:0.01 Al_2O_3:0.25 $MPP(OH)_2$:15 H_2O.

The synthesis gel was prepared by adding tetraethylorthosilicate (TEOS, 97%, Merck) and GeO_2 (99.998%, Aldrich) to an aqueous solution of the $MPP(OH)_2$ under continuous stirring and using aluminium isopropoxide (98%, Aldrich) as the Al source. The resulting mixture was kept at room temperature under continuous stirring until the desired gel composition was reached by evaporation of water and ethanol from the hydrolysis of TEOS. The gel was then autoclaved in Teflon-lined stainless steel autoclaves at 448 K for 12 days. The final solid was recovered by filtration, exhaustively washed with water and dried at 373 K overnight. The resulting ITQ-22 solid was calcined at 853 K in air in order to obtain the acid zeolite.

Samples SSZ-33 and germanium containing Beta (Beta/Ge) have been synthesized following the procedures reported in the literature [14,35]. The acid form of these samples was obtained by calcination in air at 853 K. Commercially available ZSM-5 and Beta zeolites (CBV8020 and CP811 – Beta, respectively, supplied by Zeolyst Int.) have been used to compare their catalytic behaviour with SSZ-33 and ITQ-22. CBV8020, supplied in its ammonium form, has been calcined in air at 500 °C in order to obtain the acid form. Commercial beta (CP811), supplied in its acid form, has been used without any further treatment.

2.2. Catalyst characterization

Crystallinity and phase purity of solids were determined by powder X-ray diffraction (XRD) using a Philips X'Pert diffractometer equipped with a graphite monochromator, operating at 40 kV and 45 mA and using nickel-filtered Cu Kα radiation (λ = 0.1542 nm). The chemical composition of the samples was analysed in a 715-ES ICP-Optical Emission spectrometer after dissolution of the solids in a HNO_3/HF solution. Infrared spectra were measured with a Nicolet 710 FT IR spectrometer. Pyridine adsorption–desorption experiments were carried out on self-supported wafers (10 mg cm^{-1}) of original samples previously activated at 673 K and 10^{-2} Pa for 2 h. After wafer activation, the base spectrum was recorded, and pyridine vapour (6.5×10^2 Pa) was admitted into the vacuum IR cell and adsorbed onto the zeolite. Desorption of pyridine was performed in vacuum over three consecutive 1 h periods of heating at 423, 523, and 623 K, each followed by an IR measurement at room temperature. All the spectra were scaled according to the sample weight.

Nitrogen adsorption isotherms were measured at 77 K on a Micromeritics ASAP 2010 volumetric adsorption analyser. Before the measurements, the samples were outgassed for 12 h at 673 K. The specific surface area was calculated by applying the BET model to the nitrogen adsorption data.

2.3. Reaction procedure

The catalytic alkylation of benzene with ethanol and 2-propanol was conducted in vapour phase at atmospheric pressure in a fixed-bed continuous glass down flow reactor (11 mm internal diameter) [28]. Benzene was fed in excess to the alcohol in a molar ratio of 4, while the N_2 flow was fixed to achieve a 1:10 molar ratio of N_2 to alcohol. Prior to addition of the reactants, the acid catalyst was heated to 623 K at a heating rate of 5 K/min, under a flow of nitrogen. After 30 min, the temperature was raised to 723 K and maintained at that temperature for 1 h. The reactor was then cooled to the reaction temperature (553 K).

Benzene conversion was normalized to the maximum conversion possible in the alkylation reaction taking into account that benzene was fed in excess with respect to alcohol (4:1 molar ratio).

Liquid phase alkylation of benzene with propylene was carried out with the acid zeolites, pelletized, crushed, and sieved at 0.25–0.42 mm diameter. The reaction was performed in an automated high pressure stainless steel reactor, at 3.5 MPa, 398 K, WHSV = 12 h^{-1} referred to the olefin, and benzene to propylene (B/P) molar ratio of 3.5. More details can be found in a previous study [36].

2.4. Computational details

The calculations have been performed using lattice energy minimization techniques [37,38] and the GULP code [39], employing the Ewald method for summation of the long-range Coulombic interactions, and direct summation of the short-range interactions with a cut-off distance of 12 Å. The RFO (rational functional optimizer) technique was used as the cell minimization scheme with a convergence criterion of a gradient norm below 0.001 eV/Å. A semiempirical shell model forcefield for Si/Al zeolites [40,41] has been used throughout. To account for the effect of the SDA in the system, the forcefields by Kiselev et al. [42] and Oie et al. [43] have been used for the intermolecular SDA–zeolite, SDA–SDA, and intra and intermolecular SDA interactions. For the organic dicationic SDAs, the charge distribution has been obtained by means of the Charge equilibration method [44]. In the non-neutral unit cells of composition $[Al_1Si_{111}O_{224}]$ employed to study the Si → Al substitution energy, the calculations have been performed taking into account the uniform background neutralizing charge scheme [45] that corrects the infinite terms in the Ewald summation of charged periodic systems which we have applied, as implemented in GULP. More details of the methodology can be found in previous studies [46]. The topological analysis of the window sizes associated to the oxygen atoms of the ITQ-22 has been carried out according to a ring-index topological descriptor associated to each oxygen atom as defined in previous studies [47].

3. Results and discussion

3.1. Location of the proton sites in ITQ-22 zeolite

With ITQ-22 being a recent material, the catalytic results should be discussed not only on the basis of its topology, but also on the location of the protons. The purpose of the following computer simulation is to evaluate whether there is a preferential location of the protons in the different channels of ITQ-22 zeolite.

In order to estimate the proton locations, we have used the following strategy: (i) find the minimum energy positions of the SDA dications in the micropore of ITQ-22, (ii) find the preferential location of the Al centres taking into account that they tend to locate in the minimum energy positions, and this depends on two factors: (a) the electrostatic proximity between Al (which act as 'negative' centres with respect to the Si atoms) and the positive charge of the SDA which is located around the N atoms; (b) the stability of the zeolite framework with respect to the incorporation of the Al in the 16 different T-sites. (iii) With the estimation of the probable locations of the Al atoms, we have evaluated the types of oxygen sites linked to stable Al-sites, and the location of the protons in such O-sites is compared to a topological analysis of its micropore environment in the ITQ-22 structure.

Most of the details of the calculations are given as Supplementary material, and the main conclusions are as follows. ITQ-22 contains a heterogeneous micropore space where the possible proton locations are: 8 MR, 10 MR, and 12 MR, and with the following channel intersections: 8 + 10 MR, and 10 + 12 MR, according to a previous topological analysis [48]. With the calculated most stable Al positions (T15 and T16, see SI) in ITQ-22, we then consider the oxygen atoms attached to them. There are 34 topologically distinct O-sites in ITQ-22, and we are only interested in those attached to T15 and T16, which are O22, O24, O27, O28, O32, O33 and O34, and, all together, there are 48 centres (in a unit cell of ITQ-22 comprising 112 tetrahedral atoms). By being the favourable locations for Al, these oxygens will be the possible locations of the protons, forming a Si–OH–Al15 or Si–OH–Al16 Brønsted site. The location of these protons within the channel system of ITQ-22 can be summarized as follows: 1/3 of the centres (Si9–O22–Si15 and Si12–O27–Si16) are located within 10 MR, very close to the intersection with the 12 MR channels; 1/3 of the centres (Si10–O24–Si15 and Si12–O28–Si16) are located at the intersections between 10 and 12 MR; 1/6 of the centres (Si15–O33–Si16) are located in the 12 MR; and 1/6 of the centres (Si15–O32–Si15 and Si16–O34–Si16) are located in small cavities.

3.2. Alkylation of benzene with ethanol

The alkylation of benzene with ethanol occurs through an electrophilic substitution on the aromatic ring and, likewise, it is considered to proceed via a carbenium ion-type mechanism [49–50]. The ethylation takes place by reaction of the activated alkene (formed in the case of ethanol by dehydration of the alcohol) on the acid sites of the zeolite. However, when contacting ethanol or ethylene with benzene on a solid acid catalyst, the global process can follow two major routes: (1) alkylation of benzene with ethylene producing ethylbenzene, which can undergo other consecutive alkylations yielding poly-ethylbenzenes, and (2) oligomerization of ethylene producing C4, C6 or even C8 species. The oligomers can be further transformed through cracking, isomerization and alkylation reactions, giving olefins and other alkylbenzenes (toluene, cumene, butylbenzenes, etc.). It must be remarked that, from an industrial point of view, the formation of byproducts different from diethylbenzene has a negative effect, not only on the final yield, but also on the quality of the final product [31,33].

In this part of the work we present activities and selectivities to the different products formed during the alkylation of benzene with ethanol, using ITQ-22, SSZ-33, ZSM-5 and Beta zeolites as catalysts, whose physico-chemical and acid properties are enclosed in Tables 1 and 2, respectively. In Table 1, it can be seen that although it was difficult to keep all textural and compositional characteristics of the different zeolites exactly the same, the T(IV)/T(III) ratios are very close, and the crystallite sizes of the different zeolites are not too different, specially if one takes into account differences in crystal shape. It has to be pointed out that since ITQ-22 was synthesized with Ge, we have also prepared the Beta zeolite containing Ge for comparison (Beta/Ge). If all the above-mentioned factors are accepted, then we should mainly see the effect of pore topology and proton location when comparing the activity and selectivity of the different samples presented in Table 1.

Table 1
Characteristics of samples used in this work.

Sample	ZSM-5	ITQ-22	SSZ-33	Beta/Ge
(Si + Ge)/Al molar ratio (chemical analysis)	40	37	50	50
Si/Ge ratio	–	4.8	–	16
Crystal size (μm)	0.5–1.0	0.1–0.2	0.1 × 0.1–1	0.5
Area BET (m^2/g)	386	451	490	510
Micropore volume (cc/g)	0.11	0.19	0.20	0.21

Note: Crystal size estimated from SEM pictures.

Table 2
Acid strength distribution determined by IR-pyridine measurements at different desorption temperatures of samples used in this work.

Sample	ZSM-5	ITQ-22	SSZ-33	Beta/Ge
Brönsted acidity (au) × 10^3				
423 K	157	41	112	48
523 K	126	23	109	45
623 K	66	10	50	12
Lewis acidity (au) × 10^3				
423 K	46	146	77	35
523 K	33	93	62	23
623 K	29	71	59	20

When the activity of ZSM-5 and Beta/Ge for alkylation of benzene with ethanol in gas phase is compared at 10 s time-on-stream, it can be seen (Fig. 2a) that both zeolites give high conversion of ethanol which, in all cases, is larger than the corresponding conversion of benzene (Fig. 2b). This indicates that a fraction of ethanol is converted by reactions other than alkylation, probably to give oligomerization products and coke. Nevertheless, when selectivities are compared, ZSM-5 is a much more selective catalyst than Beta/Ge zeolite for formation of ethylbenzene (EB). Since during the industrial production of EB, the diethylbenzene (DEB) formed is also transformed into ethylbenzene by transalkylation with benzene in a second reactor, we have plotted the selectivity curves for EB + DEB (Fig. 2c). It can be seen there that ZSM-5 gives, again, better selectivity than Beta, as could be expected from previous publications [28,31,51–55]. As could also be expected, Beta zeolite produces a larger amount of polyalkylated products (Fig. 2d).

A further selectivity parameter that can be useful to differentiate the catalytic behaviour of zeolites with different pore diameter is the para (p) to ortho (o) ratio in the DEB fraction. From product diffusion shape selectivity effects, one would expect that the p/o ratio would be larger in the case of the medium pore ZSM-5 than of the large pore Beta zeolite [56–58], as it is indeed found experimentally (Fig. 3, and Table 3 for detailed product distribution).

Up to this point, all results are consistent from what has been reported in the literature for alkylation of benzene with ethanol/ethylene [28,31,51–59]. However, when the alkylation of benzene with ethanol was carried out with SSZ-33 and ITQ-22, it can be seen that the activity of SSZ-33 for the conversion of ethanol and benzene is the highest among the four zeolites studied, while the activity of the others, i.e., ZSM-5, Beta/Ge and ITQ-22, is very similar (Fig. 2a and b). The highest activity of SSZ-33 could be explained on the basis of the higher amount of total Brönsted acid sites, which are able to retain pyridine at 150 °C, of this zeolite, as determined by the adsorption–desorption (see Table 2) of pyridine. Quantitative determination of the amount of Brønsted and Lewis acid sites can be derived, for instance, from the intensities of the IR bands at ca. 1450 and 1550 cm^{-1}, respectively, by using the extinction coefficients given by Emeis [60].

The Ge-containing zeolites are stable upon calcination and reaction (see XRD in Fig. S5, Supplementary material), but show a lower acid strength and a lower number of acid sites as a consequence of their lower average Sanderson electronegativity [61,62] and easier dealumination upon calcination, respectively. On the other hand, the consumption of ethanol on reactions other than benzene alkylation is lower with the Ge-containing zeolites, probably due to their lower density of acid sites.

With respect to alkylation products, it can be seen that ITQ-22 behaves like the 10 MR ZSM-5 for EB selectivity, while SSZ-33 is

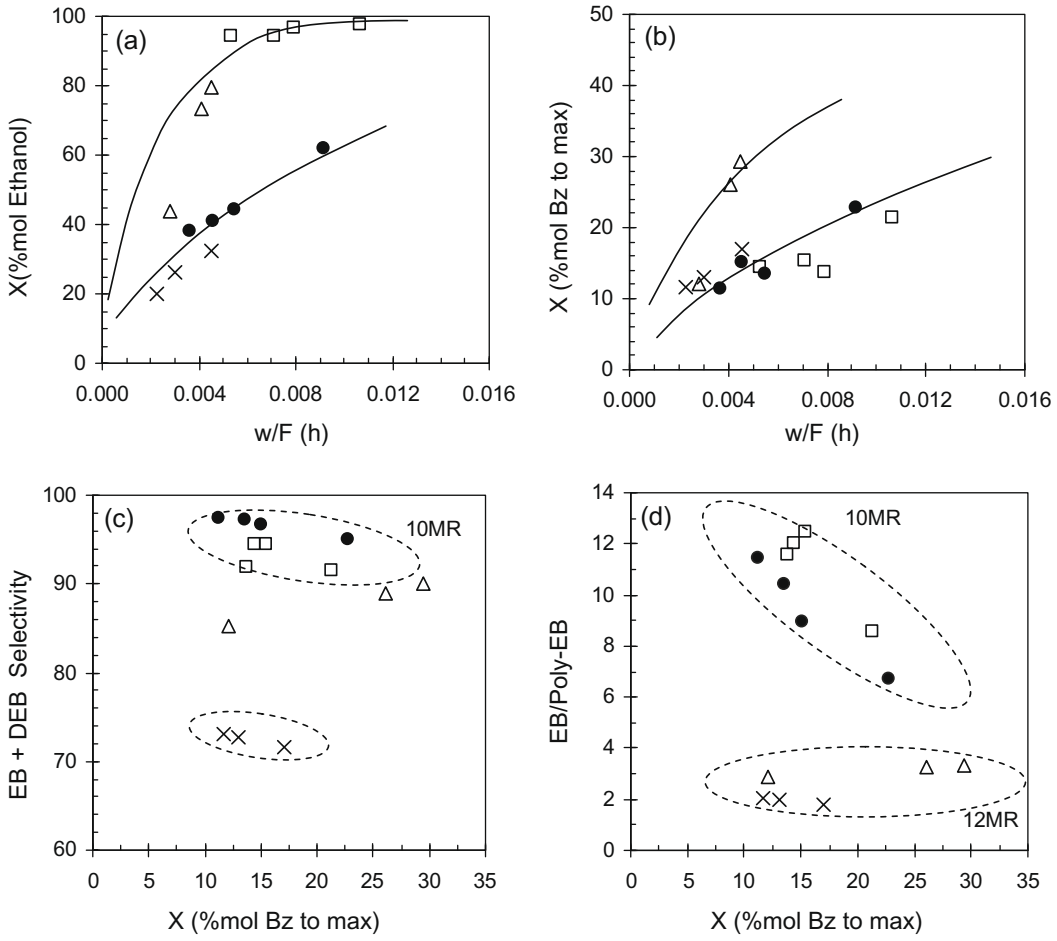

Fig. 2. Benzene alkylation with ethanol over zeolites, ZSM-5 (□), ITQ-22 (●), SSZ-33 (△) and Beta/Ge (×), at 553 K and molar ratio in feed of 4. (a) Ethanol conversion and (b) benzene conversion referred to maximum, at 10 s time-on stream, versus contact time (*w*/*F*(h)). (c) Aromatic selectivity of ethylbenzene plus diethylbenzenes (EB + DEB) and (d) ethylbenzene-to-polyethylbenzene ratio versus benzene conversion.

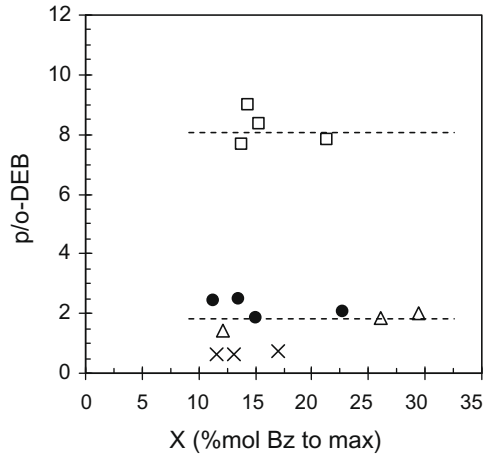

Fig. 3. Para/Ortho ratio behaviour of ZSM-5 (□), ITQ-22 (●), SSZ-33 (△) and Beta/Ge (×) zeolites for benzene alkylation with ethanol.

half way between ZSM-5 and Beta/Ge (Fig 2c and d), producing more DEB and polyalkylbenzenes with SSZ-33 than with ITQ-22. Interestingly, within the distribution of isomers in the DEB, the p/o ratio is practically the same with ITQ-22 and SSZ-33, and only slightly above that obtained with Beta/Ge (Fig. 3).

We can conclude that viz a viz ethylbenzene formation, SSZ-33 behaves closer to a 12 MR zeolite such as Beta, while the catalytic behaviour of ITQ-22 is more similar to that of ZSM-5. The reaction pattern of SSZ-33 could be explained by considering that its structure looks more like that of a zeolite with 12 MR "cavities" connected by 10 and 12 MR. Thus, the selectivity behaviour should be closer to that of a large pore zeolite with potential cage effects. In the case of ITQ-22, with discrete and connected 10 and 12 MR channels, the previous computational study indicates that a considerable amount of centres are located in 10 MR, and most of the others are located at the 12 MR (intersection between 10 × 12 MR) or near the intersection with the 12 MR. This is compatible with a catalytic behaviour of ITQ-22 similar to that of a 10 MR zeolite in ethylbenzene formation. Moreover, the presence of acid sites in the 10 × 12 MR intersections, and the possibility for the products to diffuse out of the zeolite structure through 12 MR channels can explain why the DEB isomer distribution is closer to that obtained with Beta and SSZ-33 than with ZSM-5.

In conclusion, and according to the results presented above, ITQ-22 shows, for alkylation of benzene with ethanol, a slightly higher selectivity to the formation of EB than ZSM-5 and much higher than any of the other two zeolites (Beta and SSZ-33). This indicates the predominance of the reactivity within the 10 MR or at least in the most constrained part of the 12 × 10 MR system in ITQ-22.

Besides the initial activity and selectivity of the different zeolites, we have also analysed the influence of the reaction time-on-stream (TOS) on the catalytic behaviour. The evolution of conversion with TOS is presented in Fig. 4. It is remarkable to note that

Table 3
Conversion and product distribution in benzene alkylation with ethanol and isopropanol over ZSM-5, ITQ-22, SSZ-33 and Beta/Ge samples.

Sample	Ethanol				Isopropanol			
	ZSM-5	ITQ-22	SSZ-33	Beta/Ge	ZSM-5	ITQ-22	SSZ-33	Beta/Ge
Weight catalysts – w (g × 10^3)	95.9	82.7	50.6	51.0	48.4	82.7	50.6	51.0
Benzene molar flow – F[Bz] (mol/h)	0.12	0.12	0.14	0.12	0.111	0.194	0.166	0.111
w/F[Bz] (h)	0.0106	0.0092	0.0045	0.0057	0.0056	0.0055	0.0039	0.0059
Bz conversion[a] – X (%mol Bz to max)	21.5	22.7	29.4	17.0	43.0	33.8	39.6	38.8
Alcohol conversion (%mol)	97.7	62.0	79.5	32.5	98.5	99.2	95.1	84.7
Alcohol yield in products (%)[b]								
Olefins & oligomers	52.6	24.0	22.9	8.4	30.6	47.2	40.4	37.4
Aromatics	45.1	38.1	56.5	24.1	67.9	52.0	54.6	47.2
No reaction	2.3	38.0	20.5	67.5	1.5	0.8	4.9	15.3
Aromatic product distribution[c] (%mol)								
Toluene	0.1	0.1	0.7	0.0	0.1	0.0	2.1	0.3
Ethyl-Bz	82.0	86.3	75.3	62.5	0.1	0.3	4.3	0.8
Cumene (IPB)	5.4	0.1	0.7	0.0	76.5	85.9	73.2	77.4
n-Propyl-Bz (NPB)	–	–	–	–	3.2	0.3	1.6	0.7
Buthyl-Bz	2.6	0.1	0.3	0.0	15.1	0.3	2.0	0.5
diEthyl-Bz (DEB)	9.6	8.7	14.7	9.1	–	–	–	–
triEthyl-Bz	0.0	1.9	2.3	6.1	–	–	–	–
tetraEthyl-Bz	0.0	2.0	4.9	18.6	–	–	–	–
diIsoPropyl-Bz (DIPB)	–	–	–	–	0.6	11.8	12.7	18.6
Others	0.4	0.8	1.2	3.6	4.4	1.3	4.0	1.7
Normalized dialkylated[d] (%)	Diethylbenzenes (DEB)				Diisopropylbenzenes (DIPB)			
para	54.2	30.6	28.6	21.7	68.1	34.9	32.2	32.8
meta	39.0	54.6	57.1	49.2	31.9	64.9	66.2	66.3
ortho	6.9	14.8	14.3	29.1	0.0	0.1	1.6	0.9

Note: Reaction conditions: benzene-to-alcohol molar ratio, 4; temperature, 553 K.
[a] Benzene and alcohol conversions obtained at 10 s time-on-stream.
[b] Alcohol yields directly determined by GC analysis of oligomers.
[c] Benzene free.
[d] Calculated thermodynamic equilibria at 553 K give a para/meta/ortho distribution of diethylbenzenes of 32/56.5/11.5 and of diisopropylbenzenes of 32/58.1/9.9.

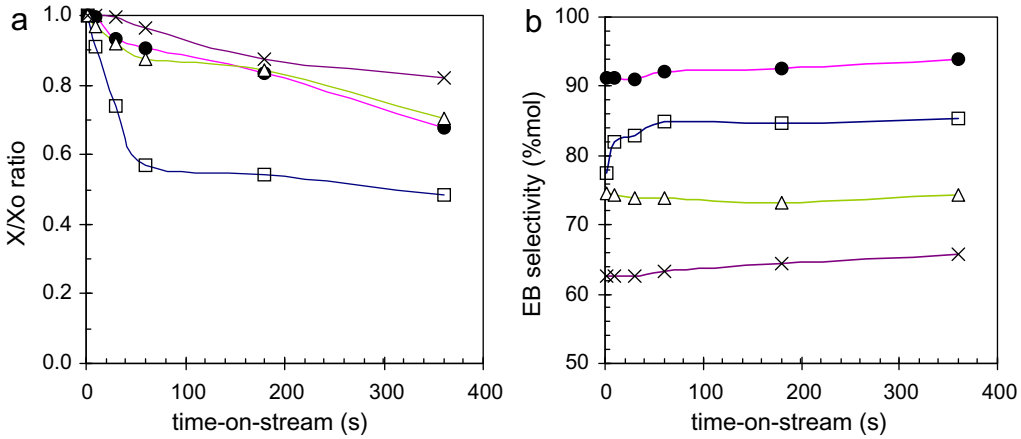

Fig. 4. Time-on-stream behaviour of ZSM-5 (□), ITQ-22 (●), SSZ-33 (△) and Beta/Ge (×) zeolites for benzene alkylation with ethanol. (a) Normalized benzene conversion referred to maximum. (b) Ethylbenzene aromatic selectivity.

ITQ-22, which behaves like a 10 MR zeolite regarding product selectivity, is considerably more stable towards deactivation than the medium pore ZSM-5, and the decrease in activity is very close to that of Beta and SSZ-33. This can be due to its lower oligomerization activity and to the pore topology with connected 10 and 12 MR channels, which will favour the diffusion of the products, increasing in this way the catalyst life (Fig. 4a), while maintaining a high selectivity to the desired EB during the whole range of time-on-stream studied (Fig. 4b).

3.3. Alkylation of benzene with isopropanol or propylene

As in the previous case with ethanol, when isopropanol or propylene is contacted with benzene in the presence of a solid acid catalyst, the alkylating agent can follow two major reaction pathways: (1) alkylation with benzene to produce cumene (IPB), which can further react to give diisopropylbenzene (DIPB); (2) oligomerization of the olefin to produce C6 and C9 olefins that can be further transformed through cracking, isomerization and alkylation giving mainly C2–C6 olefins that could also alkylate benzene and IPB [63].

Conversion of isopropanol is high for all the zeolites considered (Fig. 5a) but, as in the case of ethylbenzene production, the conversion of alcohol is higher than the conversion of benzene (Fig. 5b), indicating that other reactions such as oligomerization of propylene are also taking place.

When cumene (IPB) selectivity is considered, ITQ-22 gives higher values than Beta/Ge, ZSM-5 or SSZ-33 (see Fig. 5c). Since the

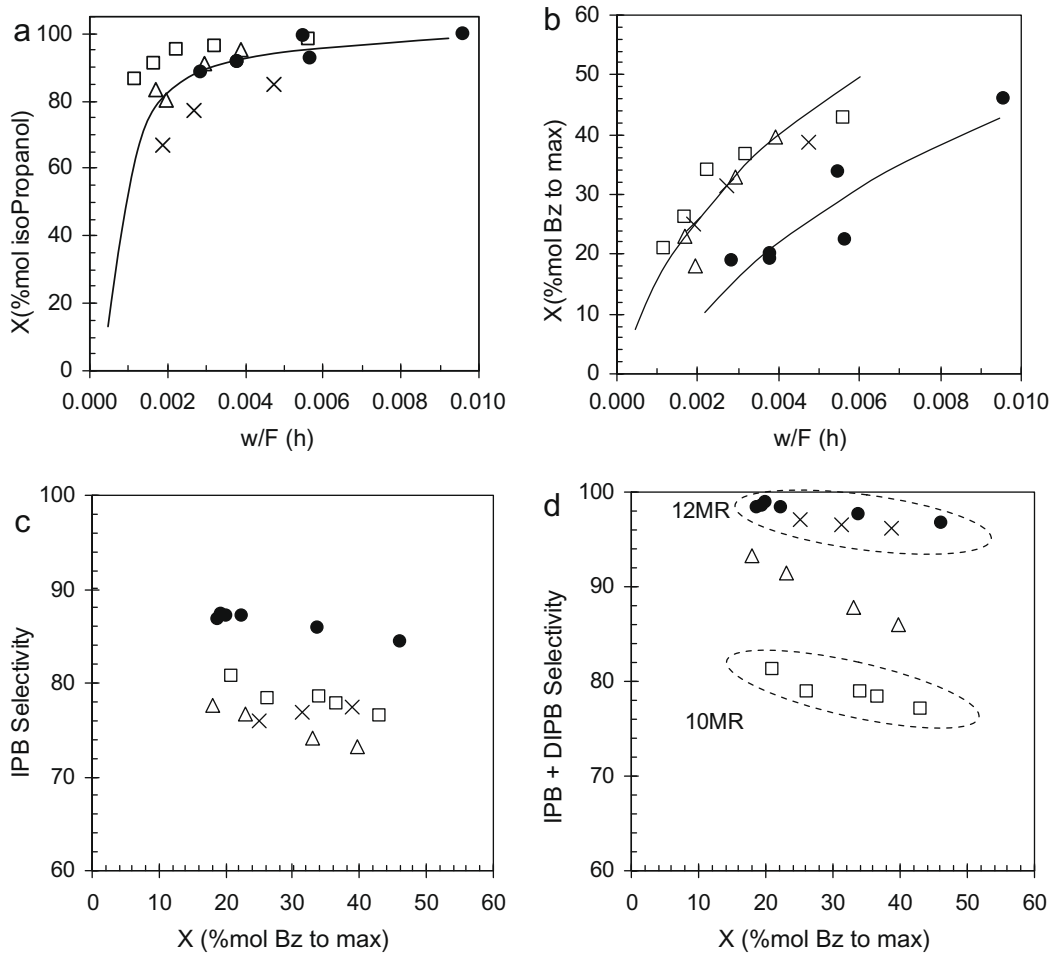

Fig. 5. Benzene alkylation with isopropanol over zeolites, ZSM-5 (□), ITQ-22 (●), SSZ-33 (△) and Beta/Ge (×), at 553 K and molar ratio in feed of 4. (a) Isopropanol conversion and (b) benzene conversion referred to maximum, at 10 s time-on stream, versus contact time (w/F(h)). (c) Aromatic selectivity of cumene (IPB) and (d) aromatic selectivity of cumene plus diisopropylbenzenes (IPB + DIPB) versus benzene conversion.

DIPB products formed are reconverted to cumene in the transalkylation units that are usually present in commercial IPB processes, it is interesting to consider the selectivity to IPB + DIPB. Fig. 5d shows that the 10 MR ZSM-5 gives the lowest value, and, interestingly, both Beta/Ge and ITQ-22 give similar values and much larger than ZSM-5. Finally, SSZ-33 gives again a selectivity value which is intermediate between that of the 10 MR ZSM-5 and the 12 MR Beta zeolite. It is most interesting to observe that ITQ-22, which reacts more like a 10 MR zeolite for the synthesis of EB + DEB during alkylation of benzene with ethanol, behaves like a 12 MR for the

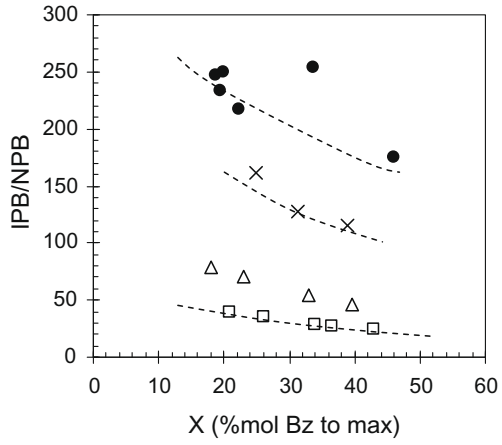

Fig. 6. Iso-/*n*-propylbenzene ratio of ZSM-5 (□), ITQ-22 (●), SSZ-33 (△) and Beta/Ge (×) zeolites, for benzene alkylation with isopropanol.

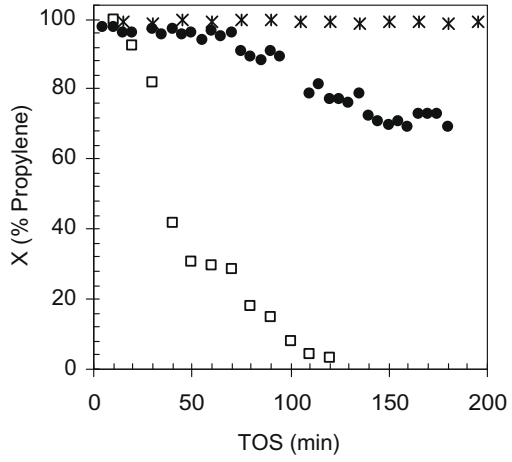

Fig. 7. Benzene alkylation with propylene over zeolites ZSM-5 (□), ITQ-22 (●) and Beta (⨯), at 398 K, 3.5 MPa, WHSV = 12 h^{-1} and molar ratio in feed of 4. Propylene conversion.

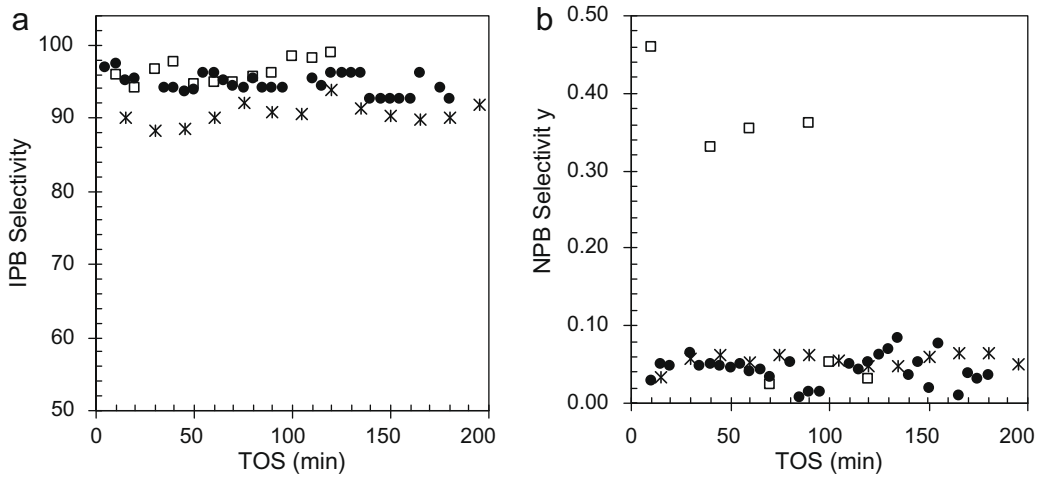

Fig. 8. Benzene alkylation with propylene over zeolites ZSM-5 (□), ITQ-22 (●) and Beta (⋇), at 398 K, 3.5 MPa, WHSV = 12 h^{-1} and molar ratio in feed of 4. (a) Selectivity to cumene (IPB); (b) selectivity to *n*-propylbenzene (NPB).

synthesis of IPB + DIPB when benzene is alkylated with isopropanol. According to the computational study, only 1/6 of the total Brönsted acid sites are located in 12 MR channels, but 1/3 of the centres are in the intersections between 10 and 12 MR. This special location can be responsible for the high selectivity of ITQ-22 to mono-alkylation to give IPB, as multiple alkylation reactions could be sterically hindered. Moreover, the rapid diffusion of the primary products through the multipore system will decrease the chances for successive alkylation reactions.

In the case of propylbenzenes, isopropylbenzene (cumene) is the major isomer though *n*-propylbenzene (NPB) is also formed. It should be remarked that in the industrial process the presence of NPB has a negative effect on yield and on the product quality. It has been reported [64,65] that NPB can be formed by transalkylation between isopropylbenzene and benzene, which is the reaction favoured with 10 MR zeolites such as ZSM-5 with respect to large pore zeolites such as Beta. This is indeed observed in our case, and the results shown in Fig. 6 indicate a lower ratio of IPB/NPB for ZSM-5 than for Beta/Ge. Interestingly, ITQ-22 gives a higher IPB/NPB ratio than the 12 MR pore Beta/Ge zeolite, while the value obtained with SSZ-33 is intermediate between ZSM-5 and Beta/Ge.

The results presented show an interesting catalytic behaviour of zeolite ITQ-22 in benzene alkylation processes, since its multipore structure gives maximum selectivity to the desired product, e.g., ethylbenzene or cumene, depending on the starting alkylating agent.

It has to be taken into account that the catalytic results presented in this work have been obtained in vapour phase. In the case of ethylbenzene production, around 50% of the commercial processes still operate in gas phase and use medium pore ZSM-5-based catalysts, although the general trend is to shift towards large pore zeolites and liquid phase processes [31]. However, in the case of cumene, the need to lower the proportion of NPB in the final product led the industry to develop liquid phase alkylation processes based on large pore zeolites such as Beta. Therefore, it is essential, from an applied point of view, to test ITQ-22 in liquid phase conditions and to compare its catalytic behaviour with the reference Beta zeolite. To do this, benzene has been alkylated with propene in liquid phase conditions (3.5 MPa and 398 K) in a stainless steel fixed-bed reactor, and the evolution of olefin conversion with time-on-stream (TOS) is shown in Fig. 7. There, ITQ-22 is compared with two commercially available zeolites (Zeolyst, Int:), a 10 MR ZSM-5 (CBV8020, Si/Al = 40) and a large pore Beta (CP811, Si/Al = 13). The behaviour of ITQ-22 is, also in this case, closer to the large pore Beta than to ZSM-5, which shows low activity due to the diffusional restrictions under these reaction conditions. Selectivity to cumene is slightly higher with ITQ-22 than with Beta, and comparable NPB levels are produced with the two zeolites (Fig. 8). Thus, ITQ-22 is also an active and highly selective catalyst for alkylation of benzene with propylene in liquid phase.

4. Conclusions

Zeolite ITQ-22, which is formed by a system of connected 8, 10 and 12 MR channels, is an active catalyst for the synthesis of ethylbenzene and cumene by alkylation of benzene with ethanol and 2-propanol in the vapour phase. In these conditions the selectivity to the desired products is higher than that obtained with the industrially used catalysts based on ZSM-5 and Beta for ethylbenzene and cumene, respectively. This high selectivity can be explained, on one hand, by the multipore structure itself, which enhances diffusion of the primary products before being involved in consecutive reactions, and on the other hand, by taking into account that according to theoretical calculations only 1/6 of the total Brönsted acid sites are located in the 12 MR channels, whereas the rest are in the intersections of the 10 and 12 MR pores, or in the 10 MR channels close to the intersections. Thus, mono- and dialkylated products are formed in the case of ethanol, and monoalkylated (IPB) product is formed in the case of isopropanol or propylene, but the formation of heavier compounds leading to a selectivity reduction and/or to catalyst deactivation is sterically hindered.

Thus, ITQ-22, with its multipore structure containing connected 10 and 12 MR pores, shows a unique behaviour as a multipurpose alkylation catalyst, not only in gas phase, but also in the liquid phase alkylation of benzene with propylene.

Zeolite SSZ-33, which could be seen as a zeolite with 12 MR "cavities" connected by 10 and 12 MR, presents an intermediate behaviour as compared to ZSM-5 and Beta.

Acknowledgments

Funding through MAT2006-14274-C02-01 (Ministerio de Ciencia e Innovación of Spain) and PROMETEO/2008/130 projects is acknowledged. GS thanks Centro de Cálculo (Universidad Politécnica de Valencia) for the use of their computational facilities, and the Distributed European Infrastructure for Supercomputing Applications (DEISA Consortium) for the provision of the ACIDFAU project. Technical assistance of J.A. Gaona and V. Clari is greatly acknowledged.

Appendix A. Supplementary material

This includes details of the computer simulations and XRD data of the ITQ-22 and Beta/Ge zeolite samples. Supplementary data associated with this article can be found, in the online version, at doi:10.1016/j.jcat.2009.08.012.

References

[1] N.Y. Chen, W.E. Garwood, Catal. Rev. – Sci. Eng. 28 (2–3) (1986) 185.
[2] G. Alberti, T. Bein, in: D.E.W. Vaughan (Ed.), Comprehensive Supramolecular Chemistry, vol. 7, Pergamon, 1996, p. 379.
[3] T.F. Degnan Jr., Top. Catal. 13 (4) (2000) 349.
[4] I.E. Maxwell, Catal. Today 1 (4) (1987) 385.
[5] A. Corma, Chem. Rev. 95 (1995) 559.
[6] H.G. Franck, J.W. Stadelhofer, Industrial Aromatic Chemistry, Springer Verlag, Berlin, 1988. p. 468.
[7] M.F. Bentham, G.J. Gajda, R.H. Jensen, H.A. Zinnen, Erdöl Erdgas Kohle 113 (1997) 84.
[8] Ch. Baerlocher, L.B. McCusker, D.H. Olson, in: Atlas of Zeolite Structure Types, sixth ed., Elsevier, 2007. <www.iza-online.org>.
[9] E.G. Derouane, Z. Gabelica, J. Catal. 65 (1980) 486.
[10] P.A. Vaughan, Acta Cryst. 21 (1966) 983.
[11] A. Corma, M. Puche, F. Rey, G. Sankar, S.J. Teat, Angew. Chem. Int. Ed. 42 (2003) 1156.
[12] W.M. Meier, Z. Kristallogr. 115 (1961) 439.
[13] M.D. Shannon, J.L. Casci, P.A. Cox, S.J. Andrews, Nature 353 (1991) 417.
[14] R.F. Lobo, M. Pan, I. Chan, H.X. Li, R.C. Medrud, S.I. Zones, P.A. Crozier, M.E. Davis, Science 262 (1993) 1543.
[15] A. Corma, F. Rey, S. Valencia, J.L. Jorda, J. Rius, Nature Mater. 2 (2003) 493.
[16] J.L. Paillaud, B. Harbuzaru, J. Patarin, N. Bats, Science 304 (2004) 990;
A. Corma, M.J. Díaz-Cabañas, F. Rey, S. Nicolopoulus, K. Boulahya, Chem. Commun. (2004) 1356.
[17] A. Corma, M.J. Diaz-Cabanas, J.L. Jorda, C. Martinez, M. Moliner, Nature 443 (7113) (2006) 842.
[18] K.P. De Jong, H.H. Mooiweer, J.G. Buglass, P.K. Maarsen, in: C.H. Bartholomew, G.A. Fuentes (Ed.), Studies in Surface Science and Catalysis, Catalyst Deactivation, Proceedings of the 7th International Symposium, vol. 111, 1997, p. 127.
[19] L. Domokos, L. Lefferts, K. Seshan, J.A. Lercher, J. Mol. Catal. A 162 (1–2) (2000) 147.
[20] G.J. Nacamuli, R.F. Vogel, S.I. Zones, US Patent 5 952 536 A (1999) to Chevron Chem. Co.
[21] J.M. Serra, E. Guillon, A. Corma, J. Catal. 227 (2) (2004) 459.
[22] J.M. Serra, E. Guillon, A. Corma, J. Catal. 232 (2) (2005) 342.
[23] A. Bhan, A.D. Allian, G.J. Sunley, D.J. Law, E. Iglesia, J. Am. Chem. Soc. 129 (16) (2007) 4919.
[24] P. Cheung, A. Bhan, G.J. Sunley, D.J. Law, E. Iglesia, J. Catal. 245 (1) (2006) 110.
[25] M. Boronat, C. Martinez-Sanchez, D. Law, A. Corma, J. Am. Chem. Soc. 130 (48) (2008) 16316.
[26] M. Moliner, M.J. Diaz-Cabanas, V. Fornes, C. Martinez, A. Corma, J. Catal. 254 (1) (2008) 101.
[27] D.L. Dorset, G.J. Kennedy, K.G. Strohmaier, M.J. Diaz-Cabanas, F. Rey, A. Corma, J. Am. Chem. Soc. 128 (27) (2006) 8862.
[28] A. Corma, V.I. Costa-Vaya, M.J. Diaz-Cabanas, F.J. Llopis, J. Catal. 207 (1) (2002) 46.
[29] F.J. Llopis, G. Sastre, A. Corma, J. Catal. 227 (1) (2004) 227.
[30] L. Forni, S. Amarilli, G. Bellussi, C. Perego, A. Carati, Appl. Catal. A 103 (1) (1993) 173.
[31] C. Perego, P. Ingallina, Catal. Today 73 (2002) 3.
[32] N.Y. Chen, W.E. Garwood, Catal. Rev. Sci. Eng. 28 (2&3) (1986) 185.
[33] T.F. Degnan Jr., C.M. Smith, C.R. Venkat, Appl. Catal. A 221 (2001) 283.
[34] C. Perego, S. Amarilli, G. Bellussi, O. Cappellazzo, G. Girotti, in: M.M.J. Treacy et al. (Eds.), Proc. 12th Int. Zeol. Conf., vol. 1, 1999, p. 575.
[35] M.A. Camblor, A. Corma, S. Valencia, J. Mater. Chem. 8 (1998) 2137.
[36] A. Corma, V. Martinez-Soria, E. Schnoeveld, J. Catal. 192 (2000) 163.
[37] C.R.A. Catlow, W.C. Mackrodt (Eds.), Computer Simulation of Solids, Lecture Notes in Physics, vol. 166, Springer, Berlin, 1982.
[38] (a) C.R.A. Catlow, A.N. Cormack, Int. Rev. Phys. Chem. 6 (1987) 227;
(b) K.-P. Schröder, J. Sauer, M. Leslie, C.R.A. Catlow, J.M. Thomas, Chem. Phys. Lett. 188 (1992) 320.
[39] (a) J.D.J. Gale, Chem. Soc. Faraday Trans. 93 (1997) 629;
(b) J.D. Gale, A.L. Rohl, Mol. Simul. 29 (2003) 291.
[40] G. Sastre, J.D. Gale, Chem. Mater. 15 (2003) 1788.
[41] G. Sastre, J.D. Gale, Chem. Mater. 17 (2005) 730.
[42] A.V. Kiselev, A.A. Lopatkin, A.A. Shulga, Zeolites 5 (1985) 261.
[43] T. Oie, T.M. Maggiora, R.E. Christoffersen, D.J. Duchamp, Int. J. Quantum Chem., Quantum Biol. Symp. 8 (1981) 1.
[44] A.K. Rappe, W.A. Goddard III, J. Phys. Chem. 95 (1991) 3358.
[45] M. Leslie, M.J. Gillan, J. Phys. C: Solid State Phys. 18 (1985) 973.
[46] (a) A. Pulido, A. Corma, G. Sastre, J. Phys. Chem. B 110 (2006) 23951;
(b) G. Sastre, D.W. Lewis, C.R.A. Catlow, J. Phys. Chem. 100 (1996) 6722;
(c) G. Sastre, C.R.A. Catlow, A. Chica, A. Corma, J. Phys. Chem. B 104 (2000) 416;
(d) G. Sastre, M.L. Cano, A. Corma, H. Garcia, S. Nicolopoulos, J.M. Gonzalez-Calbet, M. Vallet-Regi, J. Phys. Chem. B 101 (1997) 10184;
(e) A. Corma, C.R.A. Catlow, G. Sastre, J. Phys. Chem. B 102 (1998) 7085;
(f) M.J. Sabater, G. Sastre, Chem. Mater. 13 (2001) 4520;
(g) G. Sastre, A. Pulido, R. Castañeda, A. Corma, J. Phys. Chem. B 108 (2004) 8830.
[47] (a) G. Sastre, J.D. Gale, Microporous Mesoporous Mater. 43 (2001) 27;
(b) G. Sastre, A. Corma, J. Phys. Chem. B 110 (2006) 17949.
[48] G. Sastre, A. Corma, J. Phys. Chem. C 113 (2009) 6398.
[49] J.R. Anderson, T. Mole, V. Christov, J. Catal. 61 (1980) 477.
[50] Y. Du, H. Wang, S. Chen, J. Mol. Catal. A 179 (2002) 253.
[51] K.H. Chandawar, S.B. Kulkarni, P. Ratnasamy, Appl. Catal. 4 (1982) 287.
[52] P.G. Smirniotis, E. Ruckenstein, Ind. Eng. Chem. Res. 34 (5) (1995) 1517.
[53] C. Flego, G. Pazzuconi, E. Bencini, C. Perego, in: B. Delmon, G.F. Froment (Eds.), Studies in Surface Science and Catalysis, Elsevier, Catalyst deactivation, Proceedings of the 8th International Symposium, vol. 126, 1999, p. 461.
[54] J.J. Yuan, B.S. Gevert, Indian J. Chem. Tech. 11 (2004) 346.
[55] S.-J. Xie, L.-Y. Xu, Q.-X. Wang, J. Bai, Y.-D. Xu, in: E. Iglesia, J.J Spivey, T.H. Fleisch (Eds.), Studies in Surface Science and Catalysis, Natural Gas Conversion, vol. 136, 2001, p. 81.
[56] N. Arsenova-Hartel, H. Bludau, W.O. Haag, H.G. Karge, Micropor. Mesopor. Mater. 35–36 (2000) 113.
[57] R. Ganti, S. Bhatia, in: H.G. Karge, J. Weitkamp (Eds.), Studies in Surface Science and Catalysis, Zeolite Science 1994: Recent Progress and Discussions, vol. 98, 1995, p. 171.
[58] N. Arsenova-Hartel, H. Bludau, R. Schumacher, W.O. Haag, H.G. Karge, E. Brunner, U. Wild, J. Catal. 191 (2) (2000) 326.
[59] M. Raimondo, G. Perez, A. De Stefanis, A.A.G. Tomlinson, O. Ursini, Appl. Catal. A 164 (1997) 119.
[60] C.A. Emeis, J. Catal. 141 (1993) 347.
[61] R.T. Sanderson, J. Am. Chem. Soc. 105 (1983) 2259.
[62] W.J. Mortier, R.A. Schoonheydt, Prog. Solid State Chem. 16 (1985) 1.
[63] S. Siffert, L. Gaillard, B.L. Su, J. Mol. Catal. A 153 (2000) 267.
[64] J. Cejka, B. Wichterlova, Catal. Rev. Sci. Eng. 44 (3) (2002) 375.
[65] E.G. Derouane, H. He, S.B.D.A. Hamid, I.I. Ivanova, Catal. Lett. 58 (1) (1999) 1.